Int. J. Solids Structures Vol. 19, No. 10, pp. 845–856, 1983
Printed in Great Britain

0020-7683/83 $3.00 + .00
Pergamon Press Ltd

ON THE TRANSITION FROM A DIAMOND MODE TO AN AXISYMMETRIC MODE OF COLLAPSE IN CYLINDRICAL SHELLS

VIGGO TVERGAARD
Department of Solid Mechanics, The Technical University of Denmark, Lyngby, Denmark

(*Received* 15 *January* 1983; *in revised form* 23 *March* 1983)

Abstract—The influence of buckling pattern localization on the collapse mode of axially compressed elastic–plastic circular cylindrical shells is investigated. Initial imperfections are assumed to be axisymmetric and the possibility of bifurcation into a non-axisymmetric shape is analysed. For sufficiently thin-walled shells bifurcation occurs before the load maximum; but in more thick-walled shells the axisymmetric deformations are stable beyond the maximum load, at which localization into a single outward buckle takes place. It is found that localization delays bifurcation considerably, such that sufficiently thick-walled shells will collapse in an axisymmetric mode. The theoretical predictions are compared with a number of published experimental results.

1. INTRODUCTION

The collapse mode of axially compressed circular cylindrical shells made of ductile materials has been subject to a number of experimental investigations, e.g. Batterman[1], Lee[2], Horton *et al.*[3] and Johnson *et al.*[4]. All these observations show that relatively thick shells (small radius to thickness ratios) buckle axisymmetrically, whereas thinner shells buckle in a diamond pattern with a circumferential wave-number dependent on the thickness. The theoretical background of this transition from a non-axisymmetric to an axisymmetric mode of collapse has not been clear so far.

For shells with a sinusoidal axisymmetric imperfection Gellin[5] has analysed the occurrence of bifurcation into a non-axisymmetric mode. This analysis for shells compressed into the plastic range is analogous with that of Koiter[6] for elastic shells. The imperfection sensitivities predicted by Gellin[5] are in good agreement with test results, but the analyses suggest that nonaxisymmetric buckling should always be observed. These analyses were based on J_2 deformation theory (a nonlinear elastic material model).

Recently the question of bifurcation from a periodic axisymmetric pattern into an asymmetric mode has been reanalysed by Tvergaard[7], based on incremental elastic–plastic constitutive relations. Also here bifurcation is found for all shells considered, even very thick-walled shells. Thus, the discrepancy between the J_2 deformation theory predictions of Gellin[5] and the experimentally observed transition to purely axisymmetric buckling is not a result of neglecting elastic unloading in[5]. But another significant feature disclosed by the more recent analyses[7] is that for the thicker shells bifurcation occurs after the load maximum, so that the assumed periodicity of the axisymmetric pre-bifurcation solution is unrealistic.

For a wide variety of structures under compressive loading, with the common property that the applied load vs shortening curve achieves a maximum, Tvergaard and Needleman[8–10] have shown that localization of the buckling pattern will take place at the load maximum. This means that the assumption of periodic solutions in the axial direction used in previous cylindrical shell buckling analyses, e.g.[5–7], is valid before a maximum is reached; but after a maximum, localization into one or a few buckles in the axial direction must be expected. These considerations refer to a situation, in which the overall axial shortening of the shell is prescribed. If the axial load was the prescribed quantity, stability would be lost at the maximum.

The extent to which localization of the axisymmetric prebifurcation deformations affects the onset of bifurcation into a non-axisymmetric mode is investigated in the present paper. Based on the results of[7] localization is expected to play a role for the thicker shells, and the results to be presented do indicate a transition to axisymmetric collapse for sufficiently thick-walled shells. Both the influence of small geometrical imperfections and of boundary conditions are studied, and the predictions are compared with experimental results for a variety of materials.

2. BASIC EQUATIONS

The circular cylindrical shells considered have the length L, the middle surface radius R and the thickness h. A point on the middle surface is identified by the coordinates x^1 and x^2 that measure distance in the axial direction and in the circumferential direction, respectively. The displacement components are u^α on the surface base vectors and w on the outward surface normal.

The in-plane components of the Lagrangian strain tensor at distance x^3 outward from the shell middle surface are approximated by

$$\eta_{\alpha\beta} = \epsilon_{\alpha\beta} - x^3\kappa_{\alpha\beta} \tag{2.1}$$

where $\epsilon_{\alpha\beta}$ is the membrane strain tensor and $\kappa_{\alpha\beta}$ is the bending strain tensor. A nonlinear expression for $\epsilon_{\alpha\beta}$ and a linear expression for $\kappa_{\alpha\beta}$ shall be used here[11]

$$\epsilon_{\alpha\beta} = \frac{1}{2}(u_{\alpha,\beta} + u_{\beta,\alpha}) - d_{\alpha\beta}w + \frac{1}{2}a^{\gamma\delta}(u_{\gamma,\alpha} - d_{\gamma\alpha}w)(u_{\delta,\beta} - d_{\delta\beta}w) + \frac{1}{2}(w_{,\alpha} + d_\alpha{}^\gamma u_\gamma)(w_{,\beta} + d_\beta{}^\delta u_\delta) \tag{2.2}$$

$$\kappa_{\alpha\beta} = \frac{1}{2}\left[(w_{,\alpha} + d_\alpha{}^\gamma u_\gamma)_{,\beta} + (w_{,\beta} + d_\beta{}^\gamma u_\gamma)_{,\alpha} - \frac{1}{2}d_\alpha{}^\gamma(u_{\beta,\gamma} - u_{\gamma,\beta}) - \frac{1}{2}d_\beta{}^\gamma(u_{\alpha,\gamma} - u_{\gamma,\alpha})\right] \tag{2.3}$$

where $a_{\alpha\beta}$ and $d_{\alpha\beta}$ are the metric tensor and the curvature tensor, respectively, of the undeformed middle surface, and $(\ )_{,\alpha}$ denotes covariant differentiation. Greek indices range from 1 to 2, while Latin indices (to be employed subsequently) range from 1 to 3, and the summation convention is adopted for repeated indices. The stress tensor is denoted by σ^{ij} and $\dot{(\ )}$ denotes an incremental quantity.

The elastic-plastic shell material is assumed to develop a vertex on subsequent yield surfaces, as described by the J_2 corner theory proposed by Christoffersen and Hutchinson[12]. In this theory the instantaneous moduli for nearly proportional loading are chosen equal to the J_2 deformation theory moduli and for increasing deviation from proportional loading the moduli increase smoothly until they coincide with the elastic moduli for stress increments directed along or within the corner of the yield surface.

With M^0_{ijkl} denoting the deformation theory compliances, so that $\dot{\eta}_{ij} = M^0_{ijkl}\dot{\sigma}^{kl}$, and $\mathcal{M}_{ijkl}$ denoting the linear elastic compliances, the plastic part of the compliances is $C_{ijkl} = M^0_{ijkl} - \mathcal{M}_{ijkl}$. The yield surface in the neighbourhood of the current loading point is taken to be a cone in stress deviator space with the cone axis in the direction

$$\lambda^{ij} = s^{ij}(C_{mnpq}s^{mn}s^{pq})^{-1/2}. \tag{2.4}$$

Here, $s^{ij} = \sigma^{ij} - g^{ij}\sigma_k{}^k/3$ is the stress deviator tensor and g_{ij} is the metric tensor in 3-dimensional coordinates. The positive angular measure θ of the stress-rate direction relative to the cone axis is defined by

$$\cos\theta = C_{ijkl}\lambda^{ij}\dot{s}^{kl}(C_{mnpq}\dot{s}^{mn}\dot{s}^{pq})^{-1/2} \tag{2.5}$$

and a stress-rate potential at the vertex is formulated as

$$W = \frac{1}{2}\mathcal{M}_{ijkl}\dot{\sigma}^{ij}\dot{\sigma}^{kl} + \frac{1}{2}f(\theta)C_{ijkl}\dot{\sigma}^{ij}\dot{\sigma}^{kl}. \tag{2.6}$$

From this potential the strain-rate is obtained as

$$\dot{\eta}_{ij} = \frac{\partial^2 W}{\partial\dot{\sigma}^{ij}\partial\dot{\sigma}^{kl}}\dot{\sigma}^{kl} = M_{ijkl}(\theta)\dot{\sigma}^{kl} \tag{2.7}$$

with θ-dependent compliances. Since the stress-state in the shell is approximately plane, only

the in-plane stresses enter into (2.7), which is inverted to yield the plane stress incremental constitutive relations on the form

$$\dot{\sigma}^{\alpha\beta} = \hat{L}^{\alpha\beta\gamma\delta}(\theta)\dot{\eta}_{\gamma\delta} \tag{2.8}$$

The angle of the yield surface cone is specified by θ_c, so that the transition function $f(\theta)$ in (2.6) is zero for $\theta_c < \theta \le \pi$. In the total loading range, $0 \le \theta \le \theta_0$, $f(\theta)$ is unity, and in the transition region, $\theta_0 \le \theta \le \theta_c$, $f(\theta)$ is chosen to smoothly merge the deformation theory moduli with the elastic moduli in a way which ensures convexity of the incremental relation.

More detailed descriptions of the J_2 corner theory formulations in connexion with buckling analyses have been given previously [9, 7] and shall not be repeated here. All analyses in the present paper assume a totally nonlinear material response, $\theta_0 = 0$, and a rather blunt vertex specified by $(\beta_c)_{\max} = 100°$, where $\cos\beta = \dot{\sigma}_e(3\dot{s}_{ij}\dot{s}^{ij}/2)^{-1/2}$ in terms of the Mises effective stress $\sigma_e = (3s_{ij}s^{ij}/2)^{1/2}$. The uniaxial stress-strain curve is represented by a piecewise power law with continuous tangent modulus

$$\epsilon = \begin{cases} \dfrac{\sigma}{E}, & \text{for } \sigma \le \sigma_y \\ \dfrac{\sigma_y}{E}\left[\dfrac{1}{n}\left(\dfrac{\sigma}{\sigma_y}\right)^n - \dfrac{1}{n} + 1\right], & \text{for } \sigma > \sigma_y \end{cases} \tag{2.9}$$

where n is the strain hardening exponent, σ_y is the initial yield stress and E is Young's modulus.

The requirement of equilibrium is specified in terms of the principle of virtual work

$$\int_A \{N^{\alpha\beta}\delta\epsilon_{\alpha\beta} + M^{\alpha\beta}\delta\kappa_{\alpha\beta}\}\,dA = P\delta u_P \tag{2.10}$$

where A is the middle surface area and P is the total axial load at one end of the cylinder, with corresponding axial displacement u_P. At the other cylinder end zero axial displacement is prescribed. The membrane stress tensor $N^{\alpha\beta}$ and the moment tensor $M^{\alpha\beta}$ in (2.10) are taken to be

$$N^{\alpha\beta} = \int_{-h/2}^{h/2} \sigma^{\alpha\beta}\,dx^3, \quad M^{\alpha\beta} = -\int_{-h/2}^{h/2} \sigma^{\alpha\beta}x^3\,dx^3. \tag{2.11}$$

Incremental relations for $\dot{N}^{\alpha\beta}$ and $\dot{M}^{\alpha\beta}$ in terms of $\dot{\epsilon}_{\gamma\delta}$ and $\dot{\kappa}_{\gamma\delta}$ are obtained using (2.1), (2.8) and (2.11).

3. METHOD OF ANALYSIS

The nonlinear pre-bifurcation solutions are obtained numerically by a linear incremental method. The current values of the field quantities $N^{\alpha\beta}$, $M^{\alpha\beta}$, $\epsilon_{\alpha\beta}$, etc. are taken to express an approximate equilibrium state. By expanding the principle of virtual work (2.10) about this state, using (2.2) and (2.3), the equation governing the increments, $\dot{N}^{\alpha\beta}$, $\dot{M}^{\alpha\beta}$, $\dot{\epsilon}_{\alpha\beta}$, etc. is found. To lowest order this incremental equation is

$$\int_A \{\dot{N}^{\alpha\beta}\delta\epsilon_{\alpha\beta} + \dot{M}^{\alpha\beta}\delta\kappa_{\alpha\beta} + N^{\alpha\beta}[a^{\gamma\mu}(\dot{u}_{\gamma,\alpha} - d_{\gamma\alpha}\dot{w})(\delta u_{\mu,\beta} - d_{\mu\beta}\delta w)$$

$$+ (\dot{w}_{,\alpha} + d_\alpha{}^\gamma\dot{u}_\gamma)(\delta w_{,\beta} + d_\beta{}^\mu\delta u_\mu)]\}\,dA$$

$$= \dot{P}\delta u_P - \left[\int_A \{N^{\alpha\beta}\delta\epsilon_{\alpha\beta} + M^{\alpha\beta}\delta\kappa_{\alpha\beta}\}\,dA - P\delta u_P\right]. \tag{3.1}$$

The terms bracketed on the r.h.s. of (3.1) are included to prevent drifting of the solution away from the true equilibrium path.

At each stage of the fundamental axisymmetric solution the possibility of bifurcation into an asymmetric shape is investigated. The equations governing bifurcation are obtained by assuming that, corresponding to a given increment of the prescribed quantity, there are at least two distinct incremental solutions. Using the incremental version of the principle of virtual work, with $\tilde{(\ )}$ denoting the difference between the two incremental solutions, the following equation is obtained

$$\int_A \{\tilde{N}^{\alpha\beta}\delta\epsilon_{\alpha\beta} + \tilde{M}^{\alpha\beta}\delta\kappa_{\alpha\beta} + N^{\alpha\beta}[a^{\gamma\mu}(\tilde{u}_{\gamma,\alpha} - d_{\gamma\alpha}\tilde{w})(\delta u_{\mu,\beta} - d_{\mu\beta}\delta w) + (\tilde{w}_{,\alpha} + d_{\alpha}{}^{\gamma}\tilde{u}_{\gamma})(\delta w_{,\beta} + d_{\beta}{}^{\mu}\delta u_{\mu})]\}\, dA = 0 \qquad (3.2)$$

which must be satisfied by non-zero bifurcation solutions. Here, $N^{\alpha\beta}$ are the current membrane stresses in the fundamental solution.

Bifurcation modes are assumed of the form

$$\tilde{u}_1 = \tilde{U}_1 \cos\frac{mx^2}{R}, \quad \tilde{u}_2 = \tilde{U}_2 \sin\frac{mx^2}{R}, \quad \tilde{w} = \tilde{W}\cos\frac{mx^2}{R} \qquad (3.3)$$

where the circumferential wavenumber m is an integer, and the amplitude functions $\tilde{U}_1(x^1)$, $\tilde{U}_2(x^1)$ and $\tilde{W}(x^1)$ depend only on the axial coordinate. Thus, in the solution of (3.2) the wave-number m is searched that gives the first critical bifurcation point.

The integrations in circumferential direction are straightforward, both in (3.1), where the axisymmetric displacement increments are independent of x^2, and in (3.2), where the variation in circumferential direction is sinusoidal. The equations are solved approximately by the finite element method. Both the one-dimensional displacement increments $\dot{u}_1$ and $\dot{w}$ of the fundamental axisymmetric solution and the bifurcation mode amplitudes $\tilde{U}_1$, $\tilde{U}_2$ and $\tilde{W}$ are represented as Hermitian cubics within each element.

The integrals in the axial direction in (3.1) and (3.2) are evaluated numerically, using 4 point Gaussian quadrature within each element, while Simpson's rule with 7 integration points is used through the thickness. The direction of the stress-rate, defining the angle θ in the integration points, should in principle be determined by iteration at each incremental step; but instead the stress-rates computed in the previous increment are employed. Since small increments are used in the computations, this scheme leads to small errors.

The bifurcation solutions to be presented are obtained by application of a *comparison solid*, which is identified by the instantaneous moduli associated with the current values of θ on the fundamental solution. In the most common situation, where some material points are currently in the nonlinear transition range $\theta_0 < \theta < \theta_c$, this comparison solid noes not exclude earlier bifurcation in the underlying elastic plastic solid, as has been discussed in some detail in [7]. However, based on the results of [7] this comparison solid is expected to provide a good upper bound approximation of the actual first critical bifurcation point.

Bifurcations predicted by the simplest flow theory of plasticity with a smooth yield surface are much delayed relative to the J_2 corner theory predictions, particularly for thicker shells[7]. However, using the simplest flow theory in an attempt to explain the transition to purely axisymmetric buckling would hardly be realistic, since it is well known that bifurcation predictions of deformation theory are generally in much better agreement with experimental buckling loads for plate and shell structures than similar predictions based on the simplest flow theory (see Hutchinson[13]). J_2 corner theory incorporates the deformation theory moduli, as those corresponding to total loading ($\theta \le \theta_0$), into an incremental elastic–plastic law accounting for elastic unloading etc. The bifurcation predictions still depend on the parameters θ_0 and $(\beta_c)_{max}$ describing the vertex, though. For the shells with initial axisymmetric imperfections the values $\theta_0 = 0$ and $(\beta_c)_{max} = 100°$ to be used here generally result in an average somewhere between the bifurcation predictions of J_2 deformation theory and of J_2 flow theory, respectively (see[7]).

It is noted that more accurate strain measures, (2.2) and (2.3), than those of shallow shell theory are used in the present investigation, because the critical circumferential wave-numbers

in the thick-walled shells are small ($m = 3$ or even $m = 2$ are frequently found for the radius to thickness ratios considered). It has been checked that also the column buckling load ($m = 1$) for a long shell is accurately represented by the shell theory employed.

The axisymmetric imperfections to be considered in the following are chosen according to the critical buckling mode for a perfect shell, and the corresponding critical load is used for normalization. The critical stress σ_c for this axisymmetric mode and the corresponding critical half-wave length l_c are given by[7, 14]

$$\sigma_c = -\frac{\pi^2 E_1 h^2}{6 l_c^2}, \quad l_c = \pi\left[\frac{R^2h^2}{12}\right]^{1/4}\left[\frac{E_2}{E_1} - \left(\frac{E_{12}}{E_1}\right)^2\right]^{-1/4} \tag{3.4}$$

where E_1, E_2 and E_{12} denote the physical values of the plastic moduli $\hat{L}^{1111}$, $\hat{L}^{2222}$ and $\hat{L}^{1122}$, respectively, at the bifurcation point. In the elastic range the critical stress (3.4) reduces to the well-known value $\sigma_c = -\{3(1-\nu^2)\}^{-1/2} Eh/R$.

4. LOCALIZATION BEFORE BIFURCATION

The influence of buckling pattern localization shall be studied by analysing a shell with a geometrical imperfection specified as an initial normal displacement w of the form

$$w = -h\left(\bar{\xi}_1 + \bar{\xi}_2 \cos\frac{\pi x^1}{L}\right)\cos\frac{\pi x^1}{l_c}. \tag{4.1}$$

Here, L is the length of the shell segment analysed, l_c is the critical half wave length according to (3.4), and we shall choose $L = 5l_c$. The parameter $\bar{\xi}_1$ is the amplitude of an axisymmetric periodic imperfection in the shape of the critical buckling mode for a perfect shell, and $\bar{\xi}_2$ gives a modulation of this amplitude. Most of the results to be presented are obtained using 20 elements along the length L. This is expected to give good accuracy, since computations based on only 10 elements agree well with the results obtained by the finer mesh.

For the fundamental axisymmetric deformation symmetry conditions are assumed at the ends of the segment analysed

$$\left.\begin{matrix} u_1 = \Delta \\ w_{,1} = 0 \end{matrix}\right\} \text{ at } x^1 = 0, \quad \left.\begin{matrix} u_1 = 0 \\ w_{,1} = 0 \end{matrix}\right\} \text{ at } x^1 = L \tag{4.2}$$

with axial displacement Δ at one end, so that the average axial strain is Δ/L.

The bifurcation modes are mainly characterized by a circumferential waviness in regions with compressive hoop stresses. Thus, at an inward axisymmetric buckle, such as at $x^1 = 0$, where the peak compressive hoop stress occurs at the symmetry plane, the buckles are assumed symmetric about this plane

$$\tilde{U}_1 = 0, \quad \tilde{W}_{,1} = 0 \quad \text{at} \quad x^1 = 0. \tag{4.3}$$

At an outward axisymmetric buckle, such as at $x^1 = L$ (with $L = 5l_c$), the peak hoop stress at the symmetry plane is tensile, so that here the bifurcation mode amplitude is assumed to vanish according to the anti-symmetry conditions (see also[5–7])

$$\tilde{U}_2 = 0, \quad \tilde{W} = 0 \quad \text{at} \quad x^1 = L. \tag{4.4}$$

Results of some computations are shown in Fig. 1, where the load is normalized against the critical load P_c for axisymmetric buckling of a perfect shell, see (3.4). The material has an initial yield stress given by $\sigma_y/E = 0.0025$, Poisson's ratio $\nu = 0.3$, the strain hardening exponent $n = 10$, and the parameters $\theta_0 = 0$ and $(\beta_c)_{max} = 100°$ characterizing the vertex formation. The radius to thickness ratio is $R/h = 12.5$, corresponding to the most thick-walled shells analysed in [7]. The dashed curve in Fig. 1 shows a result obtained in [7] for $\bar{\xi}_1 = 0.02$ and $\bar{\xi}_2 = 0$, assuming that the axisymmetric mode remains periodic beyond the load maximum and that the bifurcation mode is periodic with the half wave length $2l_c$ in the axial direction.

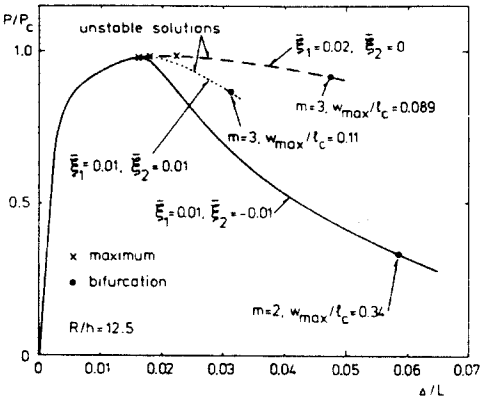

Fig. 1. Axial load vs shortening for cylindrical shells with $\sigma_y/E = 0.0025$ and $n = 10$. Solid curve and dotted curve correspond to $L = 5l_c$, while $L = l_c$ for dashed curve.

When localization of the axisymmetric buckling pattern is allowed for, either a localized outward buckle or a localized inward buckle will be expected, and small initial imperfections are chosen to enforce each situation. For $\bar{\xi}_1 = 0.01$, $\bar{\xi}_2 = -0.01$ localization in an outward buckle takes place at $x^1 = L$, whereas for $\bar{\xi}_1 = 0.01$, $\bar{\xi}_2 = 0.01$ localization occurs in an inward buckle at $x^1 = 0$. In the case of the outward buckle the solid curve in Fig. 1 shows that bifurcation is much delayed by localization and that the amplitude w_{max} of the axisymmetric buckle at bifurcation is nearly four times the value found under the assumption of periodic modes (dashed curve). However, for the inward buckle (the dotted curve) the delay is much smaller and the value $w_{max}/l_c = 0.11$ is only a little higher than that of the periodic mode. The critical circumferential wave number is $m = 2$ for the bifurcation on the solid curve, and $m = 3$ on the two other curves.

The axisymmetric middle surface deflections at bifurcation are drawn in Figs. 2(a, b) corresponding to the solid curve and the dotted curve of Fig. 1, respectively. The deflections are shown in the correct scale relative to the radius, and both sides of the prescribed symmetry plane are included in the figures. It is seen that localization does take place after the load maximum, as expected based on more general considerations[8–10]; but a repeated computation for a shell twice as long, $-L < x^1 < L$, still with the imperfections $\bar{\xi}_1 = 0.01$, $\bar{\xi}_2 = 0.01$, shows that the deformation pattern of Fig. 2(b) looses stability just before the maximum. Bifurcation of the symmetric pattern shown in Fig. 2(b) takes place at $\Delta/L = 0.017$, and subsequently only one of the two outward buckles grows into a mode quite similar with that shown in Fig. 2(a).

Thus, beyond the load maxima both the dashed curve and the dotted curve in Fig. 1 represent unstable solutions that are only obtained by prescribing symmetry requirements, which are not realistic in a long shell. The stable axisymmetric mode in a long shell after the maximum involves localization into a single outward buckle (Fig. 2a), with so small deformations outside the localized region that they are hardly visible. While the load decays, elastic

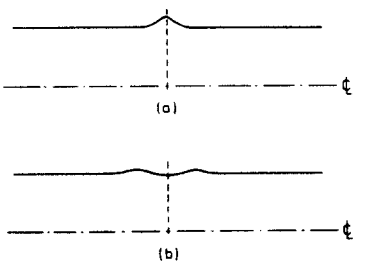

Fig. 2. Axisymmetric middle surface deflections of cylindrical shells at bifurcation, for $R/h = 12.5$, $\sigma_y/E = 0.0025$ and $n = 10$. Computations for $L = 5l_c$, with both sides of the symmetry plane drawn. (a) $\bar{\xi}_1 = 0.01$, $\bar{\xi}_2 = -0.01$. (b) $\bar{\xi}_1 = \bar{\xi}_2 = 0.01$.

unloading takes place everywhere except in the near vicinity of the growing bulge, resulting in a much stiffer material response. This stiffening effect together with the reduced compressive hoop stress beside a single buckle, relative to that between two neighbouring buckles, gives rise to the significant delay of bifurcation.

In the following two figures all results are based on the imperfections $\bar{\xi}_1 = 0.01$ and $\bar{\xi}_2 = -0.01$, which result in the stable mode of localization. Figure 3 illustrates the dependence on the radius to thickness ratio R/h for shells made of the same material with strain hardening exponent $n = 10$, also considered in Fig. 1. In the case of a relatively thin shell, $R/h = 100$, bifurcation occurs soon after localization at a small value of the axisymmetric mode amplitude w_{max}. For decreasing values of R/h the bifurcation delay increases, and at the same time the critical circumferential wave-number m decreases, as is also observed in experiments. The result shown in Fig. 3(d) for $R/h = 12.5$ is identical with the solid curve of Fig. 1.

Perhaps the value of the parameter w_{max}/l_c gives the strongest indication of the bifurcation delay. When bifurcation occurs for a small value of this parameter, as in Fig. 3(a), it seems quite plausible that this will lead to final collapse in a diamond mode. But bifurcation at a high value of w_{max}/l_c of the order of 0.2–0.3, as illustrated in Fig. 2(a), could hardly change the fact that the already well developed buckle is going to collapse completely in a shape that remains essentially asixymmetric. Whether or not bifurcation affects the mode, in which the next buckle collapses during the progressive folding up of the whole shell, could not be analysed without accounting for large rotation effects in the shell theory; but results as those shown in Fig. 3 certainly indicate a transition in the collapse mode of the first localized buckle, such that thinner shells will prefer a diamond pattern with a certain circumferential wave-number, whereas shells thicker than an R/h value slightly above 25 will form an essentially axisymmetric buckle.

Computations with periodic imperfections, $\bar{\xi}_1 = 0.02$ and $\bar{\xi}_2 = 0$, have also been performed for the shells considered in Fig. 3. In all four cases localization of the axisymmetric mode occurs immediately after the load maximum, as already mentioned in connexion with the instability of the dashed curve in Fig. 1. However, for the three thinner shells bifurcation a little before the maximum is found corresponding to small circumferential wave-numbers (e.g. $m = 3$ or 2), even though none of the bifurcation modes with axial half wave length $2l_c$ that were considered in [7] occur before the maximum. Such earlier bifurcations into modes with half wave lengths longer than $2l_c$ were also found by Budiansky and Hutchinson[15] for elastic shells. These long wave modes are no longer critical when axisymmetric localization takes place, and for the thickest shell considered, $R/h = 12.5$, they do not occur at all. This could partly explain the transition to purely axisymmetric collapse for thick shells; but in practice the required periodicity or near periodicity of the pre-bifurcation deformations will hardly be

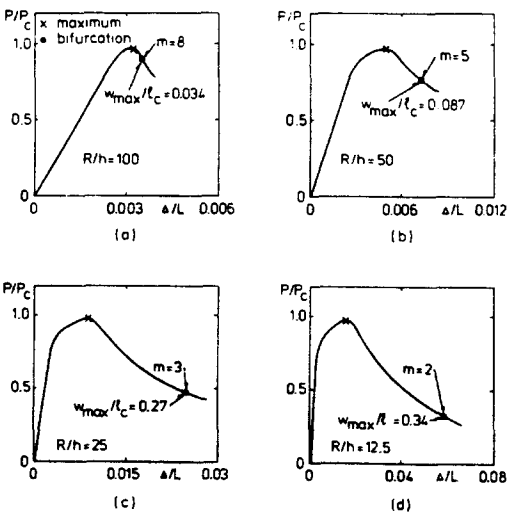

Fig. 3. Bifurcation indicated on curves of axial load vs shortening for cylindrical shells with $n = 10$. $\sigma_y/E = 0.0025$, $L = 5l_c$ and $\bar{\xi}_1 = 0.01$, $\bar{\xi}_2 = -0.01$.

common. Some kind of more localized small imperfection that triggers the mechanism discussed in relation to Fig. 3 seems more likely, and could in fact hardly be avoided.

Column buckling ($m = 1$) is also found in some of the analyses, particularly for the shells with periodic axisymmetric imperfections, where the effective bending stiffness is reduced all along the shell. However, these instabilities are not reported here, since they depend heavily on the column type boundary conditions assumed and on the total length of the shell. Naturally, the experimentally observed transition from a diamond pattern to an axisymmetric pattern refers to shells sufficiently short so that column buckling does not occur.

The degree of strain hardening of the shell material affects the bifurcations found in [7] such that a high hardening material favours bifurcation prior to the maximum more than a low hardening material. This indicates that the radius to thickness ratio R/h at the transition to purely axisymmetric buckling should be larger for a low hardening material than for a high hardening material.

In Fig. 4 a very low hardening material is considered, with strain hardening exponent $n = 100$ (nearly ideally plastic), but otherwise the same material parameters used in the previous figures. Here, the bifurcation delay is larger than found in Fig. 3; but still for $R/h = 50$ the value $w_{max}/l_c = 0.091$ at bifurcation is not very big. In Fig. 4(c) for $R/h = 25$ the delay is very large, and the axisymmetric solution reaches $w_{max}/l_c = 0.29$ at the small load $P/P_c = 0.17$ without any bifurcation. Thus, for the low hardening material Fig. 4 indicates a transition to purely axisymmetric buckling at an R/h value somewhat higher than that found in Fig. 3, but still in the range of 50–25.

5. EDGE EFFECTS

The localization considered in the previous section was assumed to be initiated by a small axisymmetric geometrical imperfection of the middle surface. Even for a completely perfect shell the critical buckling mode in the plastic range is axisymmetric and this mode too will localize at the load maximum. But in reality the influence of the boundary conditions will often act as a more dominant imperfection than small inaccuracies of the middle surface geometry.

Various edge effects, such as those resulting from clamping, from frictional support against a flat plate or from a ring stiffener, have the common feature of promoting an axisymmetric waviness near the edge. Thus the focus in the present paper on axisymmetric deformations and on the possibility of bifurcation away from these is naturally connected both with the edge effects and with the shape of the first critical buckling mode in a perfect shell.

Here a completely clamped shell will be considered in order to get some impression of the influence of edge effects. Thus, at $x^1 = L$ the boundary conditions for the fundamental axisymmetric solution are taken to be

$$u_1 = 0, \quad w = 0, \quad w_{,1} = 0, \quad \text{at} \quad x^1 = L \tag{5.1}$$

and the conditions on the bifurcation mode are taken to be

$$\left.\begin{aligned} \tilde{U}_1 = 0, \tilde{U}_2 = 0 \\ \tilde{W} = 0, \tilde{W}_{,1} = 0 \end{aligned}\right\} \quad \text{at} \quad x^1 = L. \tag{5.2}$$

At the other end, $x^1 = 0$, the symmetry boundary conditions (4.2a) and (4.3) are still employed.

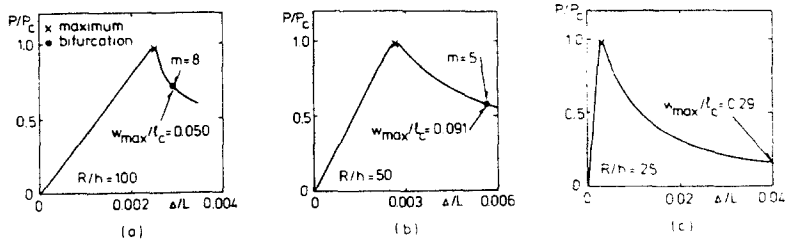

Fig. 4. Bifurcation indicated on curves of axial load vs shortening for cylindrical shells with $n = 100$, $\sigma_y/E = 0.0025$, $L = 5l_c$ and $\tilde{\xi}_1 = 0.01$, $\tilde{\xi}_2 = -0.01$.

It is noted that, in addition to an edge clamping, (5.1) and (5.2) also represent the conditions at a ring stiffener with large rigidities against bending, torsion and circumferential stretching. The shells considered are still taken to have the length $L = 5l_c$, and no initial imperfections are assumed, $\bar{\xi}_1 = \bar{\xi}_2 = 0$.

During axial compression an outward wave forms near the clamped edge, with a rather small amplitude, but large enough so that the first plastic yielding takes place here. Furthermore, the localized buckle growth after the load maximum is initiated by this edge wave, so that the effect of the edge wave is similar to that of the initial geometrical imperfection assumed in Section 4. However, with the localized axisymmetric buckle growing near the clamped edge the conditions (5.2) are a noticeable further restriction on the possible bifurcation modes. In all the cases analysed the distance between the localized wave peak and the clamped edge is very close to l_c.

Figure 5 shows results for the shell material also considered in Fig. 3, with strain hardening exponent $n = 10$. For $R/h = 100$ and $R/h = 50$ bifurcation is considerably more delayed than was found in Fig. 3, and for the thicker shells, $R/h = 25$ and $R/h = 12.5$, no bifurcation is found at all in the range considered, up to values of w_{max}/l_c beyond 0.3. The figure indicates that, with the clamped edge restrictions, the transition to purely axisymmetric collapse will take place at a radius to thickness ratio somewhat below 50.

In Fig. 6 results are shown for the very low hardening material that was considered in Fig. 4, with the strain hardening exponent $n = 100$. It is noted that the shell with $R/h = 150$ in Fig. 6(a) is thinner than any of the shells considered in Fig. 4. With the large bifurcation delay found in Fig. 6(c) the indication is that the transition to axisymmetric collapse will be located at an R/h value somewhat higher than 50.

The shell material in Fig. 7 is also very low hardening, with $n = 100$; but here the ratio of the initial yield stress to Young's modulus is given a smaller value, $\sigma_y/E = 0.001$, more representative of mild steel. Figure 7 shows that the bifurcation delay occurs at considerably thinner shells than found in Fig. 6, and for $R/h = 100$ no bifurcation is found at all up to an axisymmetric mode amplitude as large as $w_{max}/l_c = 0.3$. The figure indicates a transition to purely axisymmetric collapse at an R/h value somewhere in the vicinity of 150.

In connexion with the rather strong influence of the parameter σ_y/E, seen by comparing Figs. 6 and 7, it is noted that classical buckling in the elastic range ($|\sigma_c| < \sigma_y$ according to 3.4) requires $R/h > 242$ in a shell with $\sigma_y/E = 0.0025$, but $R/h > 605$ in a shell with $\sigma_y/E = 0.001$. For the shells made of very low hardening materials the maximum load and the corresponding buckling pattern localization occur just after initial yielding, at $P/P_c \approx 1$. Therefore, the general stress level in the vicinity of the growing localized buckle, including the compressive hoop stresses that promote bifurcation into an asymmetric mode, will be lower in a shell with a smaller value of σ_y, relative to Young's modulus E. Corresponding to this lower stress level bifurcation at a given axisymmetric mode amplitude w_{max}/l_c requires a thinner shell.

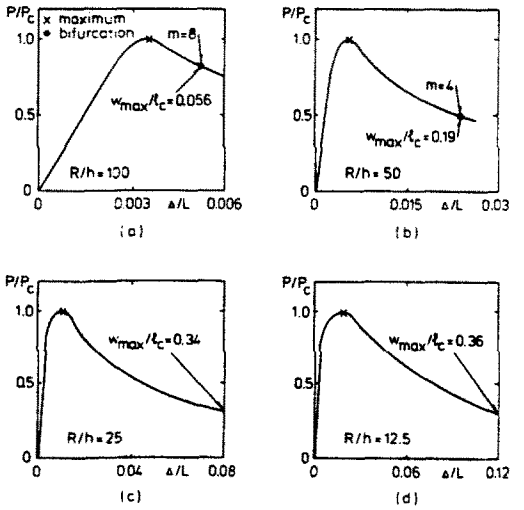

Fig. 5. Bifurcation indicated on curves of axial load vs shortening for cylindrical shells with $n = 10$, $\sigma_y/E = 0.0025$ and $L = 5l_c$. The shells are clamped at one end, with $\bar{\xi}_1 = \bar{\xi}_2 = 0$.

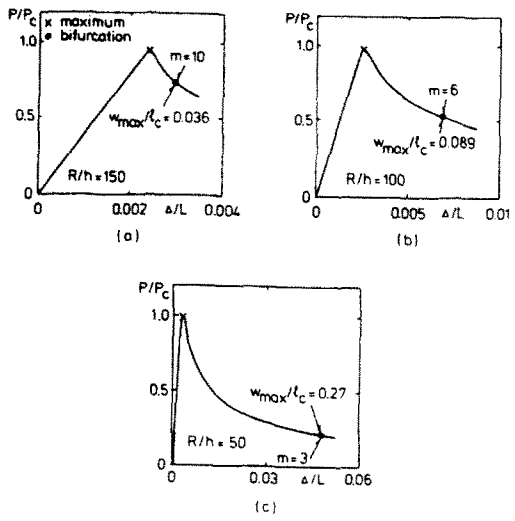

Fig. 6. Bifurcation indicated on curves of axial load vs shortening for cylindrical shells with $n = 100$. $\sigma_y/E = 0.0025$ and $L = 5l_c$. The shells are clamped at one end, with $\bar{\xi}_1 = \bar{\xi}_2 = 0$.

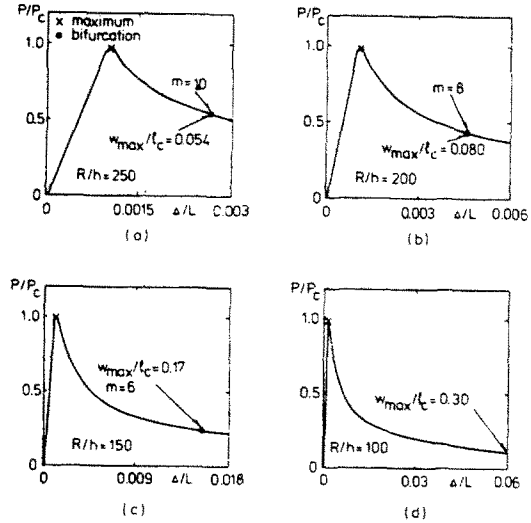

Fig. 7. Bifurcation indicated on curves of axial load vs shortening for cylindrical shells with $n = 100$. $\sigma_y/E = 0.001$ and $L = 5l_c$. The shells are clamped at one end, with $\bar{\xi}_1 = \bar{\xi}_2 = 0$.

Comparison of Figs. 5 and 6, and of Figs. 3 and 4, shows clearly that the R/h value at the transition to axisymmetric collapse is smaller for a high hardening material than for a low hardening material. But comparison of Figs. 6 and 7 indicates that the value of the parameter σ_y/E has a considerably stronger influence on the R/h value at the transition.

6. DISCUSSION

The analyses in Sections 4 and 5 show that localization of the axisymmetric buckling pattern at the load maximum has a strong influence on the occurrence of bifurcation into a non-axisymmetric mode. Previous analyses based on assuming periodic modes in the axial direction have not indicated any transition to an axisymmetric mode of collapse, even for very thick-walled shells [5, 7]; but it was noted in [7] that neglecting localization at the load maximum is not realistic. A significant result of the present investigation is that localization delays bifurcation into a diamond pattern, such that for sufficiently small R/h ratios no bifurcation is found in the range considered.

The transition indicated by the present bifurcation results, from a diamond mode of collapse in relatively thin-walled shells to an axisymmetric mode of collapse in more thick-walled shells,

refers only to the first developed buckle. If the shortening is continued after that the first buckle has folded up completely, a neighbouring wave will start to form, etc. leading to the progressive collapse observed experimentally. The distribution of negative hoop stresses around the second buckle (or a later buckle) is not identical with that around the first buckle; but the mechanisms are rather similar, with the collapsed buckle providing a rather stiff support at one end of the next growing buckle. It seems reasonable to expect that bifurcation will be prevented in all successive buckles, for a value of R/h not too much below the value leading to the transition in the collapse mode at the first buckle.

The thin shell theory employed in the present investigation, assuming small strains and moderate rotations, is not completely adequate in all the cases considered. Particularly in the most thick-walled shells analysed, the thin shell theory does not give high accuracy, and strains do not remain small. Furthermore, moderate rotations are exceeded in the final stages of the computations that are continued up to values of w_{max}/l_c as large as 0.3. However, the tendency of the bifurcation delay due to localization is clear already in the thin-walled shells, for small strains and rotations, and the transition to purely axisymmetric collapse is followed, to a large extent, within the range of validity of the theory. Therefore, it seems reasonable to state that the essential features of the problem are disclosed by the shell theory employed.

The special elastic–plastic constitutive relationship, J_2 corner theory, employed in the present investigation, is chosen because bifurcation predictions based on the simplest flow theory are generally too conservative[13]. If the simple flow theory had been applied in the present paper, instead of J_2 corner theory, bifurcation would have occurred later (see comparisons in [7]), and thus larger R/h values at the transition to axisymmetric collapse would have been predicted.

The cylindrical shells tested by Batterman[1] and by Lee[2] are made of aluminium alloys with a great deal of strain hardening and with σ_y/E around 0.004. In both series of tests a purely axisymmetric mode of collapse is observed for sufficiently small values of R/h, and a diamond shaped pattern is observed for larger values of R/h. In an intermediate range of R/h values the observed collapse modes are characterized as almost axisymmetric, as slightly ovalized in the central region along the shell, or as axisymmetric near the ends with a gentle diamond pattern on the central region. Predominantly axisymmetric patterns are observed by Batterman[1] for $R/h < 45$ and by Lee[2] for $R/h < 30$. Also Horton *et al.*[3] observe the transition of collapse modes in their aluminium cylinders at $R/h \approx 30$.

The computational results in Figs. 3 and 5 for a material with an appreciable amount of strain hardening, $n = 10$, and with $\sigma_y/E = 0.0025$ are comparable with the experimental results for aluminium cylinders in [1–3], even though no particular effort has been made to match the material parameters. The computational results indicated a transition to an axisymmetric collapse mode at a value of R/h somewhere in the range of 50–25, which seems to be consistent with the experimental observations.

Cylindrical shells made of structural steel have been considered by Sridharan *et al.*[16]. Two experiments for $R/h = 150$ show that a mild steel shell with $\sigma_y/E = 0.0012$ has developed a sharp axisymmetric outward buckle, while a shell made of high yield steel, $\sigma_y/E = 0.0015$, has developed a sequence of inward dimples around the cylinder. This is quite consistent with the computational result in Fig. 7 for a very low hardening material, $n = 100$, with $\sigma_y/E = 0.001$, where the transition to axisymmetric collapse was predicted at $R/h \approx 150$. Furthermore, comparison of Figs. 6 and 7 shows that the transition to the axisymmetric mode occurs at a smaller R/h value for a larger value of σ_y/E.

Experiments by Johnson *et al.*[4] includes a series of tests for tubes made of rigid P.V.C. (polyvinylchloride). The uniaxial stress–strain curve for this material shows an approximately elastic–perfectly plastic behaviour, with some nonlinearity prior to yielding and an effective initial yield strain, σ_y/E, as large as 0.02 or even higher. Collapse in an axisymmetric mode is only observed in very thick-walled P.V.C. tubes, with $R/h < 4$. The P.V.C. tests are not directly comparable with any of the computations in the present paper; but the tendency of the result agrees with the strong sensitivity to the value of the parameter σ_y/E, as seen by comparing Figs. 6 and 7. The R/h value at the transition to axisymmetric collapse for the low hardening materials in Figs. 6 and 7 are about 1/4 of the smallest R/h value giving classical buckling in the elastic range ($|\sigma_c| = \sigma_y$). In a shell with $\sigma_y/E = 0.02$ classical buckling in the elastic range

requires $R/h > 30$, and thus the observed value of R/h at the transition in the P.V.C. tubes is of the order of magnitude to be expected.

REFERENCES

1. S. C. Batterman, Plastic buckling of axially compressed cylindrical shells. *AIAA-J.* **3**, 316–325 (1965).
2. L. H. N. Lee, Inelastic buckling of initially imperfect cylindrical shells subject to axial compression. *J. Aerospace Sci.* **29**, 87–95 (1962).
3. W. H. Horton, S. C. Bailey and A. M. Edwards, Nonsymmetric buckle patterns in progressive plastic buckling. *Experimental Mech.* **23**, 433–444 (1966).
4. W. Johnson, P. D. Soden and S. T. S. Al-Hassani, Inextensional collapse of thin-walled tubes under axial compression. *J. Strain Analy.* **12**, 317–330 (1977).
5. S. Gellin, Effect of an axisymmetric imperfection on the plastic buckling of an axially compressed cylindrical shell. *J. Appl. Mech.* **46**, 125–131 (1979).
6. W. T. Koiter, The effect of axisymmetric imperfections on the buckling of cylindrical shells under axial compression. *Proc. Kon. Ned. Ak. Wet.* **66B**, 265–279 (1963).
7. V. Tvergaard, Plastic buckling of axially compressed circular cylindrical shells. *Int. J. Thin-Walled Structures* (1983), in press.
8. V. Tvergaard and A. Needleman, On the localization of buckling patterns. *J. Appl. Mech.* **47**, 613–619 (1980).
9. A. Needleman and V. Tvergaard, Aspects of plastic post-buckling behaviour. *Mechanics of Solids*. The Rodney Hill 60th Anniversary Volume (Edited by H. G. Hopkins and M. J. Sewell), pp. 453–498, Pergamon Press, Oxford (1982).
10. V. Tvergaard and A. Needleman, On the development of localized buckling patterns. *The Buckling of Structures in Theory and Practice* (Edited by G. W. Hunt and J. M. T. Thompson). Cambridge University Press (1983).
11. W. T. Koiter, On the nonlinear theory of thin elastic shells. *Proc. Kon. Ned. Ak. Wet.* **B69**, 1–54 (1966).
12. J. Christoffersen and J. W. Hutchinson, A class of phenomenological corner theories of plasticity. *J. Mech. Phys. Solids* **27**, 465–487 (1979).
13. J. W. Hutchinson, Plastic buckling. *Adv. Appl. Mech.* **14**, 67–144 (1979).
14. V. Tvergaard, Buckling of elastic-plastic oval cylindrical shells under axial compression. *Int. J. Solids Structures* **12**, 683–691 (1976). Errata, *ibid.* **14**, 329 (1978).
15. B. Budiansky and J. W. Hutchinson, Buckling of circular cylindrical shells under axial compression. *Contributions to the Theory of Aircraft Structures*. Presented to A. van der Neut, pp. 239–259. Delft University Press, Leyden (1972).
16. S. Shridharan, A. C. Walker and A. Andronicou, Local plastic collapse of ring-stiffened cylinders. *Proc. Inst. Civ. Engrs.* Vol. 71, pp. 341–367 (1981).